Progress in Oceanography 177 (2019) 101884

Contents lists available at ScienceDirect

Progress in Oceanography

journal homepage: www.elsevier.com/locate/pocean

Seasonal changes in plankton respiration and bacterial metabolism in a temperate shelf sea

E. Elena García-Martín[a,*], Chris J. Daniels[b], Keith Davidson[c], Clare E. Davis[d], Claire Mahaffey[d], Kyle M.J. Mayers[b,e], Sharon McNeill[c], Alex J. Poulton[b,1], Duncan A. Purdie[e], Glen A. Tarran[f], Carol Robinson[a]

[a] Centre for Ocean and Atmospheric Sciences, School of Environmental Sciences, University of East Anglia, Norwich Research Park, Norwich NR4 7TJ, UK
[b] Ocean Biogeochemistry and Ecosystems, National Oceanography Centre, Waterfront Campus, European Way, Southampton SO14 3ZH, UK
[c] Scottish Association for Marine Science, Scottish Marine Institute, Oban, Argyll PA371QA, Scotland, UK
[d] Department of Earth, Ocean, and Ecological Sciences, University of Liverpool, Liverpool L69 3GP, UK
[e] Ocean and Earth Science, University of Southampton, National Oceanography Centre Southampton, Southampton SO14 3ZH, UK
[f] Plymouth Marine Laboratory, Prospect Place, Plymouth PL1 3DH, UK

ARTICLE INFO

Keywords:
Plankton community respiration
Bacterial production
Bacterial respiration
Bacterial growth efficiency
Dissolved organic carbon
Upper/bottom mixing layers
Shelf sea

ABSTRACT

The seasonal variability of plankton metabolism indicates how much carbon is cycling within a system, as well as its capacity to store carbon or export organic matter and CO_2 to the deep ocean. Seasonal variability between November 2014, April 2015 and July 2015 in plankton respiration and bacterial (Bacteria + Archaea) metabolism is reported for the upper and bottom mixing layers at two stations in the Celtic Sea, UK. Upper mixing layer (UML, >75 m in November, 41–70 m in April and ~50 m in July) depth-integrated plankton metabolism showed strong seasonal changes with a maximum in April for plankton respiration (1.2- to 2-fold greater compared to November and July, respectively) and in July for bacterial production (2-fold greater compared to November and April). However UML depth-integrated bacterial respiration was similar in November and April and 2-fold lower in July. The greater variability in bacterial production compared to bacterial respiration drove seasonal changes in bacterial growth efficiencies, which had maximum values of 89% in July and minimum values of 5% in November. Rates of respiration and gross primary production (^{14}C-PP) also showed different seasonal patterns, resulting in seasonal changes in ^{14}C-PP:CR_{O2} ratios. In April, the system was net autotrophic (^{14}C-PP:CR_{O2} > 1), with a surplus of organic matter available for higher trophic levels and export, while in July balanced metabolism occurred (^{14}C-PP:CR_{O2} = 1) due to an increase in plankton respiration and a decrease in gross primary production. Comparison of the UML and bottom mixing layer indicated that plankton respiration and bacterial production were higher (between 4 and 8-fold and 4 and 7-fold, respectively) in the UML than below. However, the rates of bacterial respiration were not statistically different ($p > .05$) between the two mixing layers in any of the three sampled seasons. These results highlight that, contrary to previous data from shelf seas, the production of CO_2 by the plankton community in the UML, which is then available to degas to the atmosphere, is greater than the respiratory production of dissolved inorganic carbon in deeper waters, which may contribute to offshore export.

1. Introduction

Shelf seas are regions of significant primary production and carbon export from continental areas to the deep ocean (Thomas et al., 2004; Carlson et al., 2010). Particulate and dissolved organic carbon is synthesized in the upper surface layer by plankton, as well as being introduced from continental runoff and atmospheric deposition. Once in the upper mixing layer (UML), organic carbon can be consumed, transformed, or transported to depth. The amount of organic carbon annually exported from the UML depends on the efficiency of remineralization in the upper mixing layer. Between 1% and 40% of primary production is exported from the euphotic layer (Herndl and Reinthaler, 2013), with less than 5% ultimately buried in shelf sea sediments (de Haas et al., 2002). This implies high rates of respiration

* Corresponding author.
E-mail address: Enma.Garcia-Martin@uea.ac.uk (E.E. García-Martín).
[1] Current address: The Lyell Centre, Heriot-Watt University, Edinburgh EH14 4AS, UK.

https://doi.org/10.1016/j.pocean.2017.12.002

Available online 08 December 2017

also occur below the UML (Thomas et al., 2004). Despite their importance in the degradation of organic matter, and therefore export, the magnitude and variability of plankton (including both total and bacterial) respiration is much less well understood than that of phytoplankton production in coastal and shelf seas.

The Celtic Sea is a north western European shelf sea characterized by winter vertical mixing, reduced vertical mixing in spring associated with an increase in phytoplankton abundance, and thermal stratification in summer (Pingree, 1980; Joint et al., 1986). The Celtic Sea has been the subject of several physical and biogeochemical studies. The most extensive was conducted by Joint et al. (2001) and focused on plankton activity, measuring pelagic primary production, bacterial production, microzooplankton respiration and organic matter sedimentation. Since then, several studies have described the physicochemical characteristics that regulate primary production in stratified waters (Hickman et al., 2012), photoacclimation and photoadaptation by phytoplankton (Moore et al., 2006), the distribution and survival of plankton in the thermocline (Sharples, 2001), and the influence of resuspension of nutrients from sediments on plankton abundance and productivity (Davidson et al., 2013). However, despite the importance of plankton respiration and bacterial growth efficiencies (BGE, defined as bacterial production divided by the sum of bacterial production and bacterial respiration) to the transfer of organic carbon produced by phytoplankton to deeper waters (Legendre et al., 2015), plankton community respiration was not measured in any of the former studies in this region. In fact, there are relatively few studies that have directly measured the seasonal variability in plankton community respiration and bacterial growth efficiencies in temperate shelf seas (Blight et al., 1995; Serret et al., 1999; Arbones et al., 2008). These seasonal studies reported peaks in plankton community respiration in spring and summer, associated with higher phytoplankton production (Blight et al., 1995; Serret et al., 1999; Arbones et al., 2008). The close coupling between primary production and respiration implies that the synthesis of organic matter by the phytoplankton is linked with higher phytoplankton respiration and/or stimulates heterotrophic plankton community (Blight et al., 1995) and bacterial respiration (Lemée et al., 2002). Newly produced organic matter also enhances bacterial production, which drives an increase in BGE (Lemée et al., 2002; Reinthaler and Herndl, 2005).

The relative magnitude of primary production, plankton respiration and bacterial growth efficiency in the upper and bottom mixing layers of shelf seas determines the efficiency of export from the surface layers, and potential sequestration to the sediment or transfer off shelf. These metabolic processes are influenced by environmental conditions such as temperature and the availability of dissolved inorganic and organic nutrients (Elser et al., 1995; López-Urrutia and Morán, 2007; Lee et al., 2009; Kritzberg et al., 2010), but there is no clear consensus as to which environmental factors most influence the individual processes in natural waters.

The aim of this study was to quantify any difference in plankton community respiration, bacterial respiration and bacterial production rates between the upper and bottom mixing layers of the Celtic Sea in different seasons, and to assess how environmental and biological conditions (temperature, nutrient concentration, chlorophyll-*a* concentration) influence plankton respiration, bacterial metabolism and bacterial growth efficiency. Data from a central shelf station were also compared with data from a station close to the shelf edge to assess the potential influence of different ocean dynamics on plankton community respiration and bacterial metabolism.

2. Material and methods

2.1. Study site and sampling procedure

Water samples were collected during three cruises in the Celtic Sea as part of the UK Shelf Sea Biogeochemistry program (see Sharples et al., this issue). This study was conducted at two stations: one at the Central Celtic Sea (CCS, 49.39 °N latitude, 8.58 °W longitude), with a maximum depth of 143 m, and another at the Shelf Edge (CS2), a station with a maximum depth of 200 m (48.57 °N latitude, 9.5 °W longitude) (Fig. 1). CCS was sampled on 4 days in November 2014 (10th, 12th, 22nd, 25th), on 6 days in April 2015 (4th, 6th, 11th, 15th, 20th, 25th) and on 3 days in July 2015 (14th, 24th, 29th). CS2 was sampled on 2 days in November 2014 (18th, 20th), 2 days in April 2015 (10th, 24th) and once during July 2015 (19th).

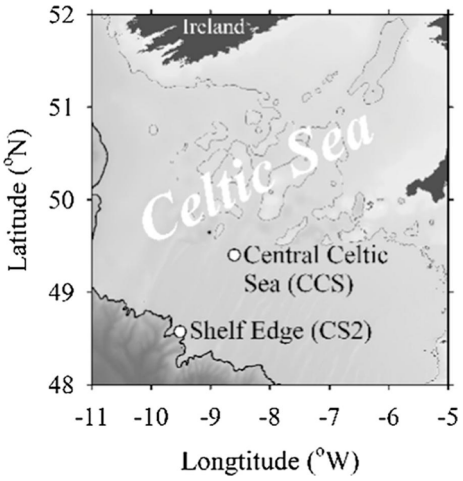

Fig. 1. Location of sampling stations (Central Celtic Sea, CCS, and Shelf Edge, CS2) in the Celtic Sea. The grey and black line represent the 100 and 200 m bathymetry contours, respectively.

At each station water samples were collected pre-dawn (~01:00–04:00 GMT) from 7 depths with 20-L Niskin bottles mounted on a sampling rosette to which was attached a conductivity-temperature-depth profiler (Sea-Bird Electronics, Washington, USA). Six of these sample depths were in the upper mixing layer (UML) at 60%, 40%, 20%, 10%, 5% and 1% of surface irradiance (I_0) (see Poulton et al., this issue). Light sampling depths were estimated by back calculation of the vertical attenuation coefficient of PAR (Kd, m^{-1}) based on either (a) assuming that the base of the thermocline was at or close to the 1% I_0 (November, April), or (b) that the sub-surface chlorophyll-*a* maximum was at or close to a depth of 5% I_0 (July) (see Hickman et al., 2012; Poulton et al., this issue). The seventh sampling depth was at 10–20 m below the base of the thermocline and within the bottom mixing layer (BML) at irradiances ≤0.1% I_0. The horizon between the UML and the BML was identified by the depth where the temperature was >0.05 °C warmer than the deepest recorded temperature in the profile (Fig. 2). Sea water was carefully decanted from the Niskin bottles into 10 L carboys for subsequent determination of plankton community respiration derived from both dissolved oxygen consumption and the reduction of 2-(ρ-iodophenyl)-3-(ρ-nitrophenyl)-5phenyl tetrazolium chloride (INT). Water samples for the determination of chlorophyll-*a* (Chl-*a*), (gross) primary production (^{14}C-PP), phytoplankton production of dissolved organic carbon (*p*DOC), bacterial production (BP) and bacterial abundance (BA) were also taken, when possible, from the same Niskin bottles (or the same depth) as the samples collected for the determination of plankton community respiration.

Water samples for determination of dissolved organic carbon (DOC) and nitrogen (DON) were collected at the same time and from the same depths, but from adjacent Niskin bottles. The full sampling procedure for the determination of nutrients and Chl-*a* concentration can be found in Hickman et al. (this issue), for bacterial abundance in Tarran et al. (this issue), and for the concentration of DOC and DON in Davis et al. (this issue). A summary of the sampling and analytical protocol is also reported here.

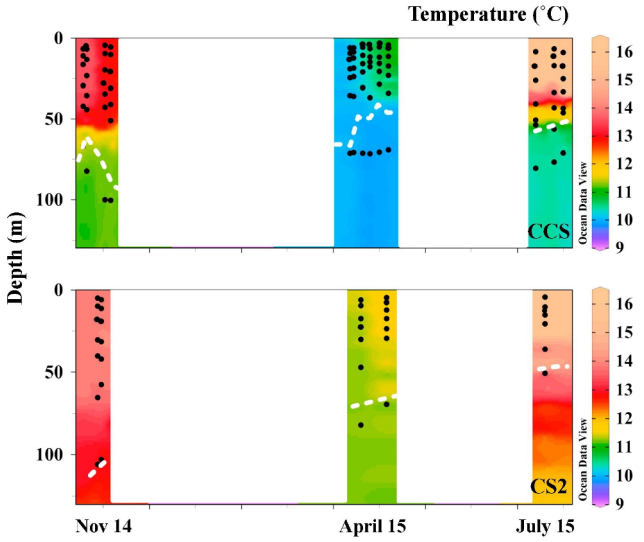

Fig. 2. Time course of the vertical distribution of temperature in the upper 130 m at CCS and CS2 during November 2014, April 2015 and July 2015. Black dots represent the depths where water was collected for measurement of plankton metabolic rates and the dotted white line is the base of the thermocline considered to be the base of the upper mixing layer.

2.2. Nutrients, total chlorophyll a and bacterial abundance

Nitrate + nitrite, ammonium, phosphate and silicate concentrations were determined using a Bran & Luebbe segmented flow colorimetric auto-analyser using classical analytical techniques as described in Woodward and Rees (2001). Water samples were collected directly from the Niskin bottles at each station. Clean sampling and handling techniques were employed, and where possible were carried out according to the International GO-SHIP recommendations (Hydes et al., 2001). Nutrient reference materials (KANSO Japan) were analysed each day to check instrument performance and to guarantee the quality of the final reported data. The typical uncertainty of the analytical results was between 2% and 3%, and the limits of detection were 0.02 μmoles L^{-1} for nitrate + nitrite phosphate and silicate and 0.03 μmoles L^{-1} for ammonium. All samples were analysed within 1–2 h of sampling.

Samples for total Chl-*a* were collected from the UML by filtering 200–250 mL of sea water through 25 mm diameter Fisherbrand MF300 or Whatman GF/F filters (effective pore size for both 0.7 μm). After filtration, pigments were extracted in 90% acetone for 18–20 h in the dark at 4 °C. Chlorophyll-*a* concentration was determined fluorometrically on a Turner Trilogy fluorometer calibrated against a pure Chl-*a* extract (Sigma) (Poulton et al., 2016; see also Hickman et al., this issue).

Samples for the enumeration of bacteria were collected from the Niskin bottles into clean 250 mL polycarbonate bottles. Subsamples were then pipetted into 2 mL microcentrifuge tubes and fixed with glutaraldehyde (50% Fisher Chemical, TEM grade, 0.5% final concentration) within 30 mins of collection. After fixing for 30 min at 4 °C, samples were stained with SYBR Green I DNA dye (Invitrogen) for 1 h at room temperature in the dark and analysed immediately for bacterial abundance (BA) by flow cytometry (Tarran et al., 2006).

2.3. Dissolved organic carbon and total dissolved nitrogen

Sea water samples for measurement of dissolved organic carbon (DOC) and total dissolved nitrogen (TDN) were collected from between 3 and 5 sampling depths which corresponded to those sampled for plankton community respiration, as detailed below. Samples were filtered through pre-combusted (450 °C) GF/F filters (Whatman, nominal pore size 0.7 μm) under low vacuum pressure (< 10 mmHg) and preserved with 20 μL of 50% (v/v) hydrochloric acid. Samples were analysed onshore using high temperature catalytic oxidation (HTCO) on a Shimadzu TOC-V_{CPN}. The limits of detection for DOC and TDN were 3.4 μmol L^{-1} and 1.8 μmol L^{-1} respectively, with a precision of 2.5%. Consensus Reference Materials from the Hansell Laboratory, University of Miami, were analysed daily with a mean and standard deviation for DOC and TDN of 43.9 ± 1.2 μmol L^{-1} (expected range 42–45 μmol L^{-1}; $n = 39$) and 32.9 ± 1.7 μmol L^{-1} (expected range 32.25–33.75 μmol L^{-1}, $n = 39$), respectively. Concentrations of dissolved organic nitrogen (DON) were determined by subtracting the concentration of inorganic nitrogen (nitrate, nitrite, ammonium) from TDN concentrations (Davis et al., this issue).

2.4. Primary production and production of dissolved organic carbon

The six sampling depths for ^{14}C-PP were all within the UML (five of which corresponded to depths sampled for plankton community respiration) and *p*DOC was measured at three of these depths. The *p*DOC depths corresponded to the depth at which surface irradiance was attenuated to 60%, 20% and 1% in November and April, and to 60%, 5% and 1% of surface irradiance in July, to account for the potential role of the sub-surface chlorophyll maximum (~5% surface irradiance; Hickman et al. 2012).

For carbon fixation and *p*DOC, water samples were collected into four 70 mL polycarbonate bottles (3 light, 1 dark), and spiked with 6–11 μCi carbon-14 labelled sodium bicarbonate (PerkinElmer Inc., specific activity 40–60 mCi/mmol). The bottles were then incubated in a purpose built constant temperature containerised laboratory at a range of seasonally adjusted irradiance levels using white-light LED light panels and neutral density filters (see Poulton et al., this issue).

On termination of the incubation, a 5 mL sub-sample from the four bottles was filtered through 25 mm 0.2 μm polycarbonate filters, with the filtrates then transferred to 20 mL scintillation vials for the determination of *p*DOC. To remove the dissolved inorganic ^{14}C, 100 μL of 50% HCl was added to each vial, which were then sealed with a gas-tight rubber septum (Kimble-Kontes) and a centre well (Kimble-Kontes) containing a CO_2 trap (consisting of a Whatman GFA filter soaked with 200 μL β-phenylethylamine). After 12 h, the CO_2 traps were removed and disposed of, and 15 mL of standard Ultima Gold™ (PerkinElmer, Inc) liquid scintillation cocktail was added to the filtrate. Spike activity was checked following Poulton et al. (2016) (see also Mayers et al. this issue) and activity in the filtrate was determined in a Tri-Carb 3100TR Liquid Scintillation Counter. Rates of *p*DOC were determined from these incubations using methods adapted from López-Sandoval et al. (2011) and Poulton et al. (2016).

The remaining 65 mL samples from the four bottles were then filtered through 25 mm 0.4 μm polycarbonate filters (Nucleopore™, USA), with extensive rinsing to remove unfixed ^{14}C-labelled sodium bicarbonate and 12 mL of standard Ultima Gold™ (PerkinElmer Inc.) liquid scintillation cocktail added. The activity on the filters was determined using a Tri-Carb 3100TR Liquid Scintillation Counter onboard. Daily rates of primary production were scaled up from short-term (6–8 h, dawn to midday) rates of carbon fixation to seasonally adjusted day lengths (9h November, 14 h April and 16 h July). These daily rates of ^{14}C-PP (see also García-Martín et al., this issue), based on short-term (< 8 h) incubations, better approximate "gross" primary production, while daily rates presented in companion papers (Mayers et al., this issue; Poulton et al., this issue; Hickman et al., this issue), based on long-term (24 h) incubations, better approximate "net" primary production (see e.g. Marra, 2002).

2.5. Respiration derived from dissolved oxygen consumption

Samples for plankton community respiration were collected from 5 depths in the UML and one depth in the BML. Plankton community respiration (CR_{O2}) was determined by measuring the decrease in

dissolved oxygen after 24 h dark bottle incubations. Dissolved oxygen concentration was measured by automated Winkler titration performed with a Metrohm 765 burette to a photometric end point (Carritt and Carpenter, 1966). Ten gravimetrically calibrated 60 mL borosilicate glass bottles were carefully filled with seawater from each 10 L carboy. Water was allowed to overflow during the filling, and care was taken to prevent bubble formation in the silicone tube. Five bottles were fixed at the start of the incubation ("zero") with 0.5 mL of 3 M manganese sulphate and 0.5 mL of 4 M sodium iodide/8 M sodium hydroxide solution (Carritt and Carpenter, 1966). The other five bottles were placed underwater in darkened temperature controlled incubators located in a temperature controlled room for 24 h ("dark"). The incubation temperatures were ±1.0 °C of the in situ temperature. Bottles were removed from the incubators after 24 h and the samples fixed as described for the "zero" bottles above. All bottles were analysed together within the next 24 h. Daily plankton community respiration was calculated from the difference in oxygen concentration between the mean ± standard error (±SE) of the replicate "zero" measurements and the mean ± SE of the replicate "dark" measurements, and is reported with ± SE. Plankton community respiration in moles of C was calculated from the CR_{O2} rates by applying a respiratory quotient of 1.

2.6. Respiration derived from INT reduction

Samples for respiration derived from INT reduction were collected from the same 6 depths as for CR_{O2}. Five 200 mL dark glass bottles were filled with seawater from each 10 L carboy. The samples in two of these bottles were immediately fixed by adding formaldehyde (2% w/v final concentration) and used as controls. All five bottles were inoculated with a sterile solution of 7.9 mM 2-(ρ-iodophenyl)-3-(ρ-nitrophenyl)-5phenyl tetrazolium chloride salt (INT, Alfa Aesar) to give a final concentration of 0.2 mM. The solution was freshly prepared for each experiment using Milli-Q water. The INT samples were incubated in the same temperature controlled incubators as the dissolved oxygen bottles for 0.5–1.4 h and then the three replicates were fixed by adding formaldehyde, as described above for the two controls. Samples were sequentially filtered through 0.8 µm and onto 0.2 µm pore size polycarbonate filters, air-dried, and stored frozen in 1.5 mL cryovials at −20 °C until further processing.

The INT reduced in each fraction (i.e. >0.8 µm and 0.2–0.8 µm) was determined from the absorbance at 485 nm of the reduced INT (formazan), extracted with propanol and measured in quartz cuvettes using a Beckman model DU640 spectrophotometer following Martínez-García et al. (2009). The mean of the INT reduction in the two controls was subtracted from the INT reduction measured in the three incubated replicates, thus correcting for any interference of the absorbance of the water due to turbidity and reduction of INT caused by non-metabolic factors (i.e. organic matter content) (average 52 ± 1% of absorbance in the incubated samples). The rate measured in the large size-fraction ($INT_{>0.8}$) will result mainly from INT reduction by eukaryotes and particle attached bacteria. By contrast, since the combined abundance of *Synechococcus* and *Prochlorococcus* made up only 1–2% of the total abundance of *Synechococcus*, *Prochlorococcus* and heterotrophic bacteria (data not shown), the main respiring organisms in the small size-fraction ($INT_{0.2–0.8}$) are expected to be free-living heterotrophic bacteria. The total plankton community respiration (INT_T) is calculated as the sum of the INT reduction in the two size fractions ($INT_{0.2–0.8}$ and $INT_{>0.8}$).

Time-course experiments were carried out on seawater collected from 5 m on the 11th November 2014, 4th April 2015 and 14th July 2015 in order to determine the optimal incubation time for INT reduction. The maximum incubation time before the INT became toxic for the plankton (seen as a decrease in the INT reduction rate due to the negative effect on cell activity of the intracellular deposition of formazan) was found to be 2, 0.8 and 0.5 h, in November, April and July respectively. Hence, all our incubations were undertaken for shorter times than these (<1.4 h < 0.8 h, <0.5 h, respectively).

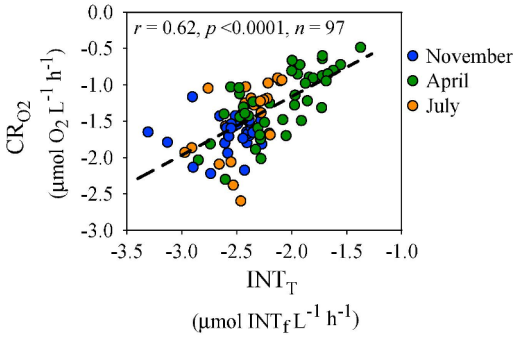

Fig. 3. Paired measurements of log-transformed plankton community respiration derived from 24 h rates of oxygen consumption (CR_{O2}) and <1.5 h rates of INT reduction (INT_T) determined from samples collected at CCS and CS2. The different colours correspond to the different months sampled: November in blue, April in green and July in orange. The dashed line corresponds to the ordinary least-squares linear relationship. The statistical Spearman correlation analysis is shown.

INT reduction was converted into dissolved oxygen consumption using the equation: Log O_2 = 0.80Log INT_T + 0.45 derived from the comparison of CR_{O2} and INT_T rates from this study (R^2 = 0.43, p < .0001, n = 97, Fig. 3). Bacterial respiration in moles of C was calculated from the INT_T reduction rates converted into units of dissolved oxygen consumption, multiplying by the $\%INT_{0.2–0.8}$ and applying a respiratory quotient of 1.

2.7. Bacterial production and bacterial growth efficiency

Water samples for bacterial production (BP) were collected from the same 6 Niskin bottles as the samples for determination of plankton community and bacterial respiration detailed above, into 125 mL acid washed polycarbonate bottles. Two stocks solutions of ^{14}C leucine (GE Healthcare UK Ltd.) were used: 11.8 GBq/mmol, 318 mCi/mmol and 11.3 GBq/mmol, 306 mCi/mmol. Aliquots of 10 µL ^{14}C leucine working solution (0.04 MBq mL^{-1}) were pipetted into 2 mL sterile centrifuge tubes with 1.6 mL of sample water and mixed. For each depth, duplicate samples were incubated for 0, 1, 2 and 3 h in the dark at temperatures representative of the depth of collection. Samples were fixed with 80 µL of 20% paraformaldehyde (final concentration of 1%). The duplicate samples were filtered onto 0.2 µm polycarbonate filters pre-soaked in 1 mM non-labelled leucine on top of a 25 mm GF/F filter as a backing filter. Each 0.2 µm polycarbonate filter was placed into a scintillation vial, dried overnight at room temperature in a fume-hood and mixed with 4 mL of Optiphase Hi-Safe II scintillation fluid. Radioactivity in the samples was measured using a Beckman Coulter LS6500 liquid scintillation counter. Bacterial population growth (cells m^{-3} d^{-1}) was calculated from ^{14}C leucine incorporation using a theoretical approach assuming no isotope dilution (Kirchman, 2001).

Cell-specific bacterial production and respiration were calculated by normalizing BP and $INT_{0.2–0.8}$ to BA, respectively. Bacterial carbon demand (BCD) was calculated as: BP + $INT_{0.2–0.8}$ and bacterial growth efficiency (BGE) as: BP/BCD.

2.8. Data analysis

Depth-integrated Chl-*a*, ^{14}C-PP, CR_{O2}, INT_T, $INT_{>0.8}$, $INT_{0.2–0.8}$ and BP rates were calculated by trapezoidal integration of the volumetric rates measured in the UML. The standard errors (± SE) of the integrated rates were calculated following the propagation procedure for independent measurements described by Miller and Miller (1988). The depth-integrated contribution of the 0.2–0.8 µm fraction to total plankton community respiration ($\%INT_{0.2–0.8}$) was calculated as the depth-integrated $INT_{0.2–0.8}$ divided by the depth-integrated INT_T and multiplied by 100.

Statistical analyses were performed with SPSS statistical software on log-transformed data where necessary. A two-way ANOVA was used to determine the effects of month and station and any interacting effects between these two factors on BA, CR_{O2}, INT_T, $INT_{0.2–0.8}$, $\%INT_{0.2–0.8}$ and BP. Non parametric t-tests were performed to verify significant differences between BA, $CR_{O2,}$ $INT_{0.2–0.8}$, $\%INT_{0.2–0.8}$, BP, cell-specific $INT_{0.2–0.8}$ and cell-specific BP in the UML and BML. Due to the low number of measurements made per month at CS2 (≤ 2), statistical tests were only performed on data from CCS. Spearman non-parametric correlation tests were used to determine the relationship between volumetric BA, CR_{O2}, INT_T, $INT_{0.2–0.8}$, BP, BCD and BGE and between each of these and environmental parameters (temperature, nitrate + nitrite concentration, ammonium, phosphate concentration, silicate concentration, Chl-*a* concentration and *p*DOC). Non-parametric multivariate techniques were used with the PRIMER v 6.1 statistical package to discern station grouping based on the plankton autotrophic metabolic rates (^{14}C-PP, *p*DOC), plankton heterotrophic metabolic rates (CR_{O2}, $INT_{>0.8}$, $INT_{0.2–0.8}$, $\%INT_{0.2–0.8,}$ and BP) and to relate these to the environmental data (temperature, nitrate + nitrite, ammonium, phosphate, silicate concentration, Chl-*a*, bacterial abundance, DOC and DON concentration). First, in order to be able to compare the data from the different months which had different mixing depths, the UML depth-integrated rate was divided by the depth of integration to derive the rate per cubic metre (weighted metabolic rate). Then, a Bray-Curtis similarity matrix was constructed from the standardized data of the plankton weighted metabolic parameters and Euclidean distances were calculated on the normalized environmental data. Sampling days were classified using distance based redundancy analysis (dbRDA) (Legendre and Anderson, 1999). A distance-based linear model (distLM) was used to analyse the relationships between plankton metabolism and environmental parameters.

3. Results

3.1. Hydrographic conditions

A full description of the hydrographic and nutrient conditions present in the Celtic Sea during the sampling period (November 2014, April 2015 and July 2015) is reported in Poulton et al. (this issue), Humphreys et al. (this issue) and Wihsgott et al. (this issue) with a brief overview given in Table 1.

The seasonal variability in hydrography followed the typical progression for temperate shelf seas. November was characterized by thermal homogeneity of the upper 55 m of the water column with weak stratification occurring in deeper waters (Fig. 2). These conditions are typical for a late summer-early autumn situation when the complete disruption of the summer thermocline has not yet occurred. During November, UML temperatures were 12–14 °C and salinity was slightly lower at the surface than in deeper waters (difference < 0.1). There was a weak thermocline at the beginning of April at 65 m which strengthened by the end of April (Table 1, Wihsgott et al. this issue). Temperatures in April (ranging from 9.8 to 11.2 °C) were lower than in November (11.2–13.7 °C), with warmer waters at the surface and colder waters at depth. Thermal stratification prevailed during July with sea surface temperatures >15.5 °C in the UML, and <11.5 °C in the BML. In November, the UML extended to 92 m at CCS and to 119 m at CS2. In April there was a shallowing of the UML from 65 m on 4th April to 45 m on 25th April at CCS, while the UML was at 65–70 m deep at CS2. In July, the UML occurred between 50 and 56 m at both stations.

3.2. Community respiration measured by dissolved oxygen consumption versus INT reduction

There was a significant correlation between oxygen consumption (μmol O_2 L^{-1} d^{-1}) and INT reduction (μmol INT_f L-1 h^{-1}) measured during the three months ($r = 0.62$, $p < .0001$, $n = 97$, Fig. 3). However, there were differences in the magnitude of the rates derived from the two methods. The difference between vertical profiles of oxygen consumption measured in November and July is greater than the difference between vertical profiles of INT reduction measured in the same months (Supp. Fig. 1). These dissimilarities could be due to several reasons. The two methods measure over different time scales (<1.4–24 h), so that any change in grazing pressure due to enclosure in relatively small bottles, could lead to a greater increase in bacterial abundance over the longer incubation times required for CR_{O2} than those for INT_T. The different time scales might also lead to differences in community structure and therefore respiration. However, the relationship between paired community respiration measurements (CR_{O2} and INT_T) in their original units indicated that there was no statistical difference between the slope of the paired measurements in April and July (Clarke test, $p = .23$: Clarke, 1980) (Fig. 3), although the slope of the data collected in November differed from that collected in April and July (Clarke test, $p < .001$). The dissimilarity between the slopes of November CR_{O2}:INT_T data and April and July CR_{O2}:INT_T data may be caused by the high variability in the low rates measured in November, the small range of CR_{O2} and INT_T rates measured in November, or the change in plankton community composition with different plankton having different abilities to take up INT. Due to the low number of data collected in each month, a single CR_{O2}:INT_T conversion model was derived from data collected in all three months (see Section 2.6) (Fig. 3).

3.3. Vertical profiles of chlorophyll-a and bacterial abundance

In general the vertical profile of Chl-*a* was characterized by a homogenous vertical distribution in November, a high subsurface Chl-*a* concentration (60–20% I_0) and decrease at deeper depths in April, and development of a subsurface peak at a depth of 5% $I_{0,}$ ~45 m in July

Table 1
Surface environmental conditions (average ± standard error) and the depth of the base of the thermocline at the Central Celtic Sea (CCS) and Shelf Edge (CS2) stations in November 2014, April 2015 and July 2015.

	November 2014		April 2015		July 2015	
	CCS	CS2	CCS	CS2	CCS	CS2
SST (°C)	13.3 ± 0.18	14.01 ± 0.13	10.49 ± 0.2	11.5 ± 0.15	16.46 ± 0.22	16[a]
Salinity	35.39 ± 0.01	35.57 ± 0.01	35.33 ± 0.01	35.59 ± 0.01	35.42 ± 0.02	35.54[a]
Nitrate + nitrite (μM)	2.11 ± 0.14	3.03 ± 0.46	3.19 ± 0.95	7.16 ± 1.06	<0.02	<0.02[a]
Ammonium (μM)	0.14 ± 0.02	9.09 ± 0.01	0.10 ± 0.02	0.09 ± 0.05	0.06[a]	0.1[a]
Phosphate (μM)	0.19 ± 0.01	0.25 ± 0.03	0.30 ± 0.06	0.45 ± 0.06	0.07 ± 0.01	0.07[a]
Silicate (μM)	0.93 ± 0.06	1.35 ± 0.04	2.55 ± 0.08	2.73 ± 0.4	0.36 ± 0.17	0.2[a]
Chlorophyll-a (μg L^{-1})	1.53 ± 0.09	0.84	3.51 ± 0.92	1.55 ± 0.72	0.29 ± 0.02	0.92[a]
Bacterial abundance (x10^6 cells mL^{-1})	0.7 ± 0.1	0.5 ± 0.1	1.0 ± 0.1	0.5 ± 0.1	0.8 ± 0.1	1.4[a]
Thermocline (m)	75 ± 7	114 ± 5	54 ± 4	67 ± 2	53 ± 2	50[a]

[a] Indicates there was only one datum for the analysis.

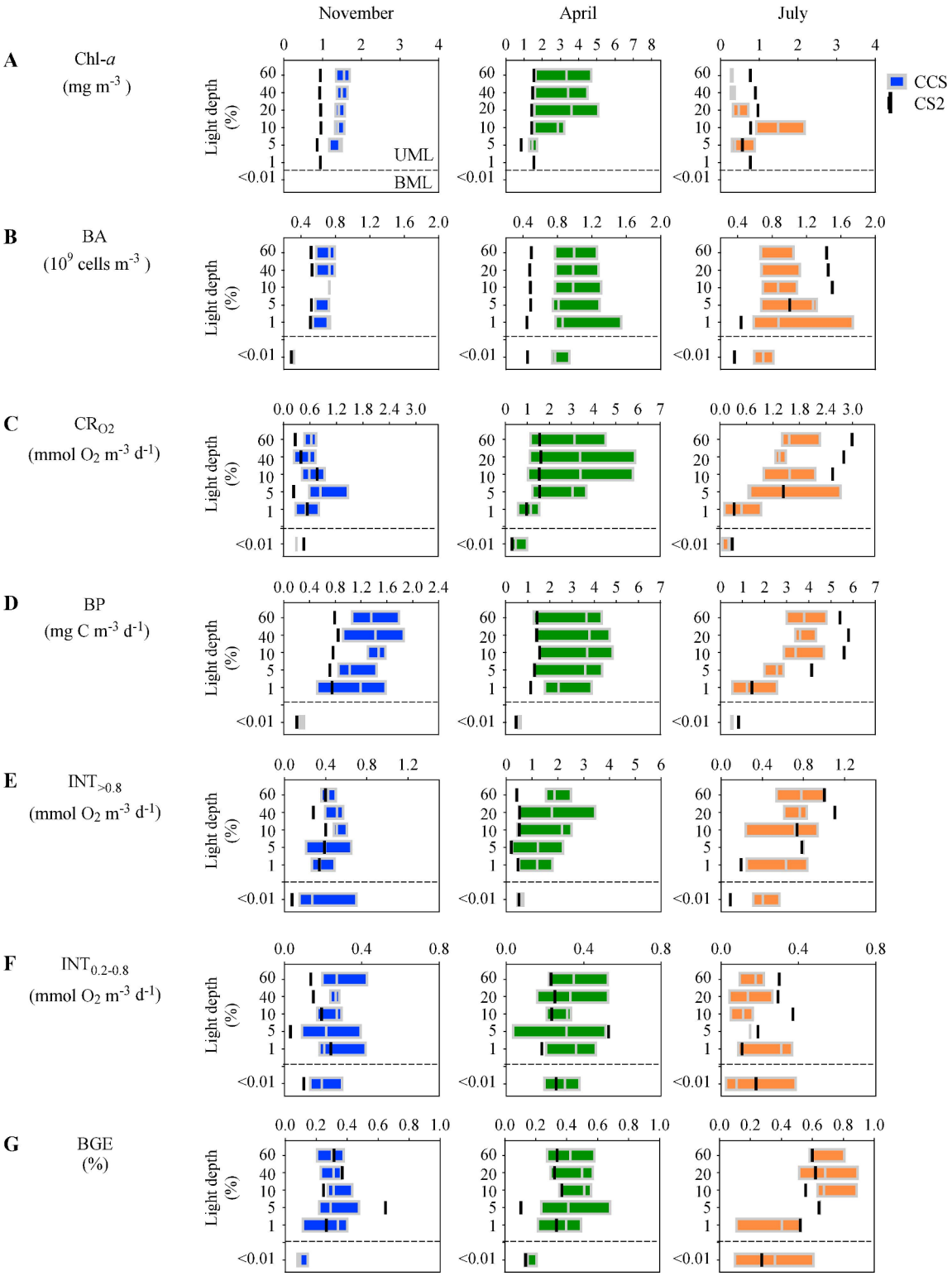

Fig. 4. Box plots of (A) Chlorophyll-*a* (Chl-*a*), (B) bacterial abundance (BA), (C) plankton community respiration derived from oxygen consumption (CR_{O2}), (D) bacterial production (BP), (E) respiration of the plankton fraction >0.8 μm ($INT_{>0.8}$), (F) bacterial respiration ($INT_{0.2–0.8}$), and (G) bacterial growth efficiency (BGE) at CCS (coloured box) and CS2 (black line) in November 2014 (blue), April 2015 (green) and July 2015 (orange).

(Fig. 4A). April had the highest Chl-*a* concentration and variability as a consequence of the development of the spring bloom.

BA varied little with depth in November and April in the UML. However, BA had a subsurface maximum at 5–1% I_0 (>44 m) at CCS in July while a homogenous distribution was observed in surface waters (60–10% I_0, 4–15 m) and a pronounced decrease in bacterial abundance occurred in deeper waters at CS2 (Fig. 4B). Bacterial abundance was significantly higher in the UML than in the BML in November, while no significant difference was observed in April and July ($p > .05$) at CCS.

3.4. Vertical profiles of plankton metabolism

The depth distribution at the two stations was similar for both CR_{O2} and BP. CR_{O2} and BP had a homogenous vertical distribution during November in the UML, with higher rates occurring in the subsurface layers (60–5% I_0, 6–24 m) than at the 1% I_0 in April, whereas CR_{O2} and BP gradually decreased from the surface (60–5% I_0, 7–50 m) to the base of the euphotic layer (considered as the layer between the surface and the depth at which incident irradiance is 1% I_0) in July (Fig. 4C and D). The vertical distribution of CR_{O2} was a result of the vertical distribution of the respiration of the >0.8 μm size fraction as free-living bacterial respiration ($INT_{0.2–0.8}$), showed a more homogenous vertical distribution at both stations in the three months (Fig. 4E and F). Overall, bacteria had similar growth efficiencies throughout the water column in November and April, while higher growth efficiencies were measured in the subsurface layers (60–5% I_0, 6–24 m) compared to the 1% I_0 depth in July. CR_{O2} in the UML was significantly higher than in the BML in April and July ($p < .014$) but not in November, while BP was significantly different in the UML and BML in the three months ($p < .002$).

In contrast to BP, $INT_{0.2–0.8}$ and the percentage of plankton community respiration attributable to bacteria were not significantly different above and below the thermocline in any month ($p > .05$). In addition, there was no significant difference between UML and BML cell-specific bacterial respiration in any month ($p > .05$, data not shown), which indicates that lower bacterial numbers in the BML sustained lower bacterial respiration rather than lower cell-specific rates. Bacterial growth efficiencies in the UML were significantly higher ($p < .007$) than in the BML in November and April but not in July due to the high variability observed in the BML during this month (Fig. 4G).

3.5. Integrated Chl-a and bacterial abundance in the upper mixing layer

There were no significant differences between the depth-integrated Chl-*a* and BA at CCS and CS2 in any of the three months, although higher Chl-*a* and BA were observed at CCS than at CS2 in April (Fig. 5 A-B). There was a seasonal evolution in the UML depth-integrated Chl-*a* with intermediate concentrations in November (monthly average 59.2 ± 5.4 mg C m^{-2}), maximum concentration in April (monthly average 80.7 ± 12.87 mg C m^{-2}) and lowest concentrations in July (monthly average 24.5 ± 3.5 mg C m^{-2}) (Fig. 5A). Depth-integrated bacterial abundance did not show any seasonal variability due to the high variability observed between days (Fig. 5B).

3.6. Integrated metabolic rates in the upper mixing layer

The two-way ANOVA comparison between the depth-integrated metabolic rates measured at the two stations in the three months indicated that, in general, there were no significant differences between CCS and CS2, but there were differences between months. The high variability between the rates measured at CCS, especially in April when there was a sharp increase in plankton metabolism related to the bloom transition period, and the low amount of data collected at the CS2 station may have contributed to the lack of any significant difference between stations.

Depth-integrated rates of CR_{O2} varied seasonally by 1.2–2.8-fold, with the lowest rates in November (monthly average 47.8 ± 5.2 mmol O_2 m^{-2} d^{-1}) and the highest rates in April (monthly average 94.9 ± 16.4 mmol O_2 m^{-2} d^{-1}) associated with the spring bloom (Fig. 5C). Depth-integrated $INT_{0.2–0.8}$ was highest and most variable in April (monthly average 18.9 ± 2.9 mmol O_2 m^{-2} d^{-1}) and significantly lower in July (monthly average 9.1 ± 0.8 mmol O_2 m^{-2} d^{-1}) (Fig. 5D). There was a clear seasonal difference in the percentage of plankton community respiration attributable to bacteria (%$INT_{0.2–0.8}$), with higher proportions in November (monthly average 37.9 ± 2.2%) than in April (monthly average 26.4 ± 4.3%) and July (monthly average 21.2 ± 3%) (Fig. 5E). Depth-integrated BP progressively increased up to 2-fold from the lowest rates in November (monthly average 6.5 ± 0.8 mmol C m^{-2} d^{-1}) to the highest rates in July (monthly average 17.7 ± 1.1 mmol C m^{-2} d^{-1}) (Fig. 5F).

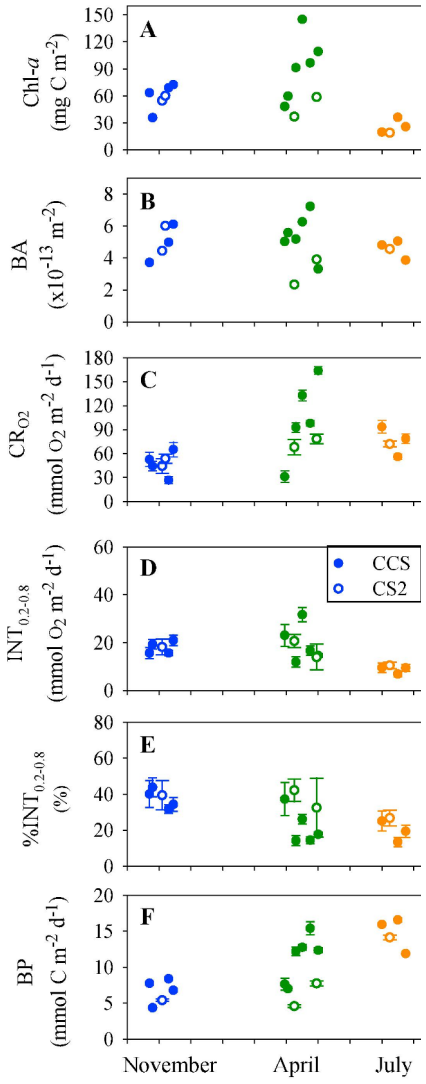

Fig. 5. Upper mixing layer depth-integrated (A) Chlorophyll-*a* (Chl-*a*), (B) bacterial abundance (BA), (C) plankton community respiration (CR_{O2}), (D) bacterial respiration ($INT_{0.2–0.8}$), (E) proportion of plankton community respiration attributable to bacteria (% $INT_{0.2–0.8}$) and (F) bacterial production (BP) at CCS (solid circles) and CS2 (open circles) during November 2014 (blue), April 2015 (green) and July 2015 (orange). Error bars represent the standard error.

3.7. Plankton metabolism and relationships with physical, chemical and biological parameters

The correlation matrix of the volumetric variables (Table 2) shows how plankton community respiration and bacterial production and respiration were related differently to the physicochemical and biological characteristics of the water column. Volumetric CR_{O2}, $INT_{0.2–0.8}$ and BP were all positively correlated to total Chl-*a* concentration and bacterial abundance. The negative correlations observed between CR_{O2}, BP and nitrate + nitrite are likely caused by the covariation between depth and nitrate + nitrite, as deep waters below the productive UML had higher nitrate + nitrite concentration and lower respiration rates due to lower Chl-*a* and bacterial abundance. Surprisingly, dissolved organic carbon produced by phytoplankton (*p*DOC), which is an indicator of the amount of substrate (DOC) available to the bacteria, was positively

Table 2
Spearman correlation matrix between volumetric bacterial abundance (BA), plankton community respiration (CR_{O2}, and INT_T), bacterial respiration ($INT_{0.2–0.8}$), bacterial production (BP), bacterial carbon demand (BCD) and bacterial growth efficiency (BGE) with environmental parameters (temperature, T; chlorophyll-*a*, Chl-*a*; nitrate + nitrite, ammonium, silicate and phosphate concentration and phytoplankton DOC production, *p*DOC). Bold numbers indicate significant relationships and $^{*}p < .05$; $^{**}p < .01$; $^{***}p < .001$.

	T	Chl-*a*	Nitrate + nitrite	Ammonium	Silicate	Phosphate	*p*DOC	CR_{O2}	INT_T	$INT_{02–08}$	$\%INT_{02–08}$	BP	BCD
BA	**−0.57****	**0.38****	**−0.42*****	0.50	−0.11	**−0.32****	**0.49****	**0.48*****	**0.72*****	**0.28****	**−0.47*****	**0.67*****	**0.62*****
CR_{O2}	−0.04	**0.40*****	**−0.32****	0.17	−0.12	**−0.40*****	**0.53*****		**0.62*****	0.17	**−0.48*****	**0.75*****	**0.60*****
INT_T	**−0.36*****	**0.54*****	**−0.39*****	0.05	0.01	**−0.26***	**0.64*****	**0.62*****		**0.55*****	**−0.45*****	**0.63*****	**0.79*****
$INT_{02–08}$	**−0.42*****	**0.38*****	−0.12	0.01	**0.21***	0.09	0.13	0.17	**0.55*****		**0.40*****	0.12	**0.75*****
$\%INT_{02–08}$	−0.04	−0.21	**0.31*****	−0.10	0.14	**0.34****	**−0.62*****	**−0.48*****	**−0.45*****	**0.40*****		**−0.51*****	−0.06
BP	0.15	**0.34****	**−0.68*****	**0.35*****	**−0.48*****	**−0.69*****	**0.59*****	**0.75*****	**0.63*****	0.12	**−0.51*****		**0.70*****
BCD	−0.19	**0.42*****	−0.12	0.16	−0.13	**−0.36*****	**0.47****	**0.60*****	**0.79*****	**0.75*****	−0.06	**0.70*****	
BGE	**0.37*****	−0.04	**−0.53*****	**0.30*****	**−0.51*****	**−0.64*****	**0.43****	**0.52*****	**0.22***	**−0.48*****	**−0.75*****	**0.75*****	0.16

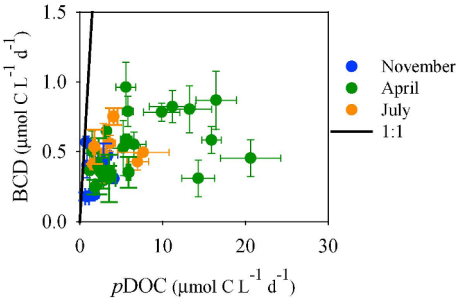

Fig. 6. Volumetric bacterial carbon demand (BCD) versus dissolved organic carbon produced as a result of phytoplankton photosynthesis (*p*DOC) during November 2014 (blue), April 2015 (green) and July 2015 (orange). The straight line is the 1:1 line. Error bars represent the standard error.

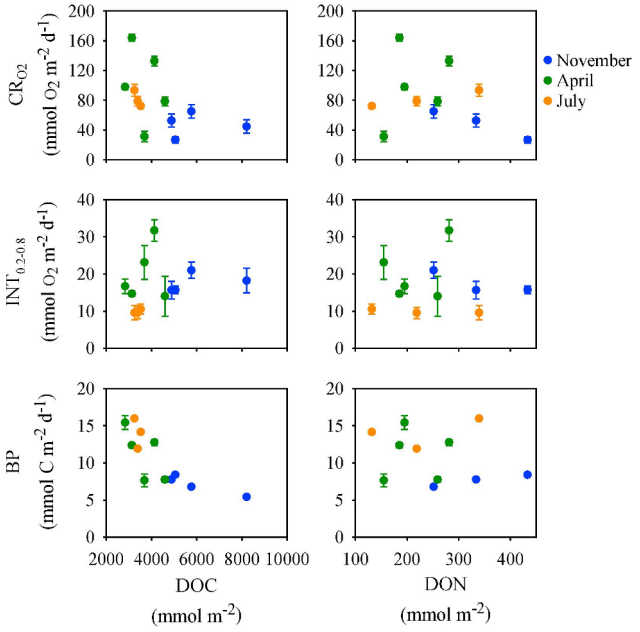

Fig. 7. Relationship between UML depth-integrated plankton community respiration (CR_{O2}), bacterial respiration ($INT_{0.2–0.8}$) and bacterial production (BP) and the concentration of dissolved organic carbon (DOC) and nitrogen (DON). Error bars represent the standard error.

correlated with plankton community respiration, bacterial production and bacterial abundance, but not with bacterial respiration. Bacterial carbon demand in the UML was lower than *p*DOC during all three months (Fig. 6).

UML depth-integrated CR_{O2}, $INT_{0.2–0.8,}$ and BP exhibited different correlations with UML depth-integrated dissolved organic carbon and nitrogen (DOC and DON) concentrations. CR_{O2} and BP were negatively correlated to DOC ($r = -0.71$, $p = .08$, $n = 12$ for CR_{O2}; and $r = -0.80$, $p < .001$, $n = 12$ for BP) while $INT_{0.2–0.8}$ was not significantly related to DOC, and there were no significant correlations between DON and any of the metabolic rates (Fig. 7).

Ordination analysis of the environmental parameters and metabolic rates provides a better understanding of the relationships between the environmental data (weighted UML depth-integrated temperature, nitrate + nitrite, phosphate, silicate, ammonium, DOC and DON concentration, Chl-*a* and bacterial abundance) and plankton metabolism during the different months. The analysis was performed separately on the weighted UML depth-integrated autotrophic (^{14}C-PP, *p*DOC) and heterotrophic (CR_{O2}, $INT_{>0.8,}$ $INT_{0.2–0.8}$,$\%INT_{0.2–0.8}$, and BP) planktonic metabolic rates. Results from this analysis indicated that 47% of the variability in plankton autotrophic responses and 81% of the variability in plankton heterotrophic responses could be explained by two axes. The environmental variables that best explained the plankton autotrophic metabolic rates were a combination of temperature and nitrate + nitrite concentration (Fig. 8A). By contrast, temperature, nitrate + nitrite, ammonium and silicate better described the plankton heterotrophic metabolic rates (Fig. 8B), which combined accounted for 100% of the fitted model variation. The ordination analysis of the autotrophic metabolic rates separated all April data at CCS from the other sampling days. Within the heterotrophic metabolic rates, three groups could be observed: Group I consists of the majority of the April data (11th, 15th, 20th and 25th April) at CCS, Group II is formed by all July data (both CCS and CS2), and Group III consists of November data together with the April data at CS2 and data collected on the 4th April at CCS.

4. Discussion

4.1. Central Celtic Sea versus shelf edge

Recent studies in the Celtic Sea have demonstrated differences in the physicochemical properties between the central Celtic Sea and the shelf edge (Sharples et al., 2001, 2009). The shelf edge station (CS2) in our study is characterized by higher turbulent mixing which supports a phytoplankton community dominated by larger cells (>20 µm), whereas phytoplankton in the central Celtic Sea are dominated by smaller cells (2–20 µm) (Sharples et al., 2009; Hickman et al., 2012; Hickman et al., this issue). In the present study, water column stratification differed between the CCS station and the shelf edge CS2 station. In April and July, there was a well-defined UML and BML separated by a thin thermocline at CCS while at CS2 the thermal gradient was less distinct and occurred over a broader depth interval (data not shown). There were, therefore, differences in the depth of the UML between the two stations (deeper at CS2 than at CCS in November and April) and in the depth of the Chl-*a* subsurface maximum (deeper at CCS than at CS2), which drove changes in the vertical distribution of plankton community respiration and bacterial production. However, these differences in hydrodynamic conditions were not reflected in differences in UML depth-integrated CR_{O2}, $INT_{0.2–0.8}$ or BP. The lack of difference in the depth integrated rates between stations may be caused by the

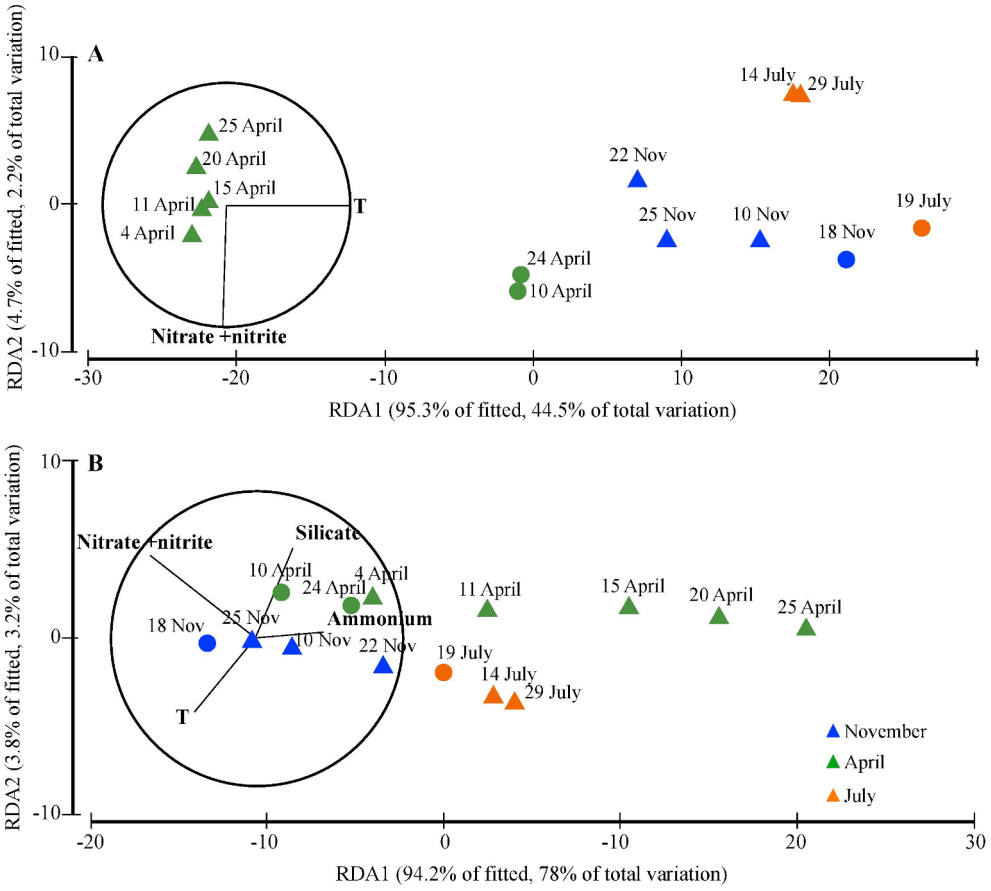

Fig. 8. Distance-based redundancy analysis (dbRDA) of the linear model describing the relationships between environmental variables (temperature, T; nitrate + nitrite concentration; silicate concentration; ammonium concentration, bacterial abundance; chlorophyll-*a*; dissolved organic carbon and nitrogen and (A) weighted depth-integrated (UML-depth integrated rates divided by the mixing layer depth) autotrophic metabolic rates (primary production and production of dissolved organic carbon) and (B) weighted depth-integrated heterotrophic metabolic rates (plankton community respiration derived from dissolved oxygen consumption, respiration of the >0.8 μm size fraction, bacterial respiration, contribution of bacterial respiration to total plankton respiration and bacterial production). Sampling days at CCS are represented by triangles and at CS2 by circles in November (blue), April (green) and July (orange). Significant environmental variables explaining the variability of the ordination (best selection procedure) are represented by the lines. Note that 12th November 2014, 6th April 2015 and 24th July 2015 data are not included due to lack of DOC and DON data for the analysis.

difference in the depth of integration, which was 30 m and 13 m deeper at CS2 than at CCS in November and April, respectively. In fact, the ordination analysis that compares the weighted plankton metabolic rates at the different stations indicated that the plankton metabolism in April at CS2 was more similar to that in November at CCS. In April, the higher increase in CR_{O2} at CCS than at CS2 may be related to the different Chl-*a* concentrations measured at the two stations (94 ± 15 and 48 ± 11 mg Chl-*a* m^{-2}, respectively). At CCS, thermal stratification developed as a consequence of the warming of surface waters, contributing to ideal conditions (increase in stability and irradiance along with high nutrient concentrations) for phytoplankton growth leading to the spring bloom (Wihsgott et al., this issue). In contrast, at CS2 the hydrodynamic conditions did not promote a sharp increase in phytoplankton growth and therefore there was a lower increase in Chl-*a* concentration, plankton community respiration and bacterial production. In fact, UML depth–integrated CR_{O2} and BP at CS2 in April were similar to the pre-bloom condition at CCS in spring and to the rates measured in November at both stations.

The higher BP rates at CCS than at CS2 in April contrast with a previous study in the Celtic Sea in April 1987 where the BP was 2-fold higher in the mixed water at the shelf edge than in the stratified waters of the continental shelf (Martin-Jézéquel and Videau, 1992). Mixing conditions are usually associated with inputs of nutrients from deep waters that can sustain plankton production. Although in our study, CCS became stratified and CS2 had a deeper mixing layer in April, nutrients were not depleted to limiting levels at either of the two stations during our sampling periods. In addition, the bacterial abundance data indicated that bacteria were not restricted by grazing as their numbers increased during April except on the last day at CCS when their abundance was reduced to values lower than at the beginning of April (Fig. 4B). This may indicate that grazing (or advection) was only important at the end of the April sampling period at CCS but not at the beginning. Therefore, the differences between our study and the Martin-Jézéquel and Videau (1992) study could be related to the different influence of the environmental conditions. Overall, strong internal waves and tidal mixing (Pingree et al., 1983; Sharples et al., 2009) can establish differences in phytoplankton distribution (Sharples et al., 2009) but not in the plankton metabolism, except in April when the earlier stratification of the water column promotes an earlier increase in plankton abundance (in terms of Chl-*a* concentration and bacterial numbers) in the Celtic Sea. Therefore, the amount of carbon cycling is similar in the inner Shelf Sea and at the shelf edge apart from April when more carbon can be exported to deeper areas or sustain higher bacterial and zooplankton activities.

4.2. Carbon metabolism of plankton communities

Rates of CR_{O2} measured during this seasonal study lie within the range of previous measurements made in the Celtic Sea (Robinson et al., 2009) and other North Atlantic shelf seas (Blight et al., 1995; Serret et al., 1999; Arbones et al., 2008) (Supplementary Table 1). Our range of $INT_{0.2–0.8}$ (0.03–0.85 μmol O_2 L^{-1} d^{-1}) corresponds with bacterial respiration rates measured in a seasonal study in the open Mediterranean Sea (Lemée et al., 2002) and lies at the lower end of the rates measured in the North Sea (Reinthaler and Herndl, 2005) and in a seasonal study in the northwest coastal region of the Mediterranean Sea (Alonso-Sáez et al., 2008). Our UML depth-integrated BP is between 8 and 50-fold greater than the euphotic depth-integrated BP measured in the Celtic Sea by Joint and Pomroy (1987) yet is 3-fold lower than BP measured by Davidson et al. (2013) in July 2008 in the area around CCS (49.8 °N, 7.8 °W). The difference between our measurements and those of Joint and Pomroy (1987) is likely caused, at least in part, by the different methodologies used (thymidine uptake versus leucine uptake). Bacterial production derived from thymidine and leucine

assimilation can be different because the leucine to thymidine incorporation ratio is not constant (Li et al., 1993; Pomroy and Joint, 1999). In fact, a leucine and thymidine incorporation comparative study performed off the Oregon coast reported 10-fold differences in the leucine and thymidine incorporation for bacterial cells (Longnecker et al., 2006). This large difference between rates due to different methods complicates direct comparison between our study and that of Joint and Pomroy (1987). During July 2015 the difference between the euphotic layer and the UML ranged between 3 and 4 ms, so the difference in the depth of integration (euphotic depth versus the UML depth) is unlikely to be the cause of the discrepancy between Davidson et al. (2013) and our data. In addition, the leucine methodology and the isotope dilution factor were similar for the two studies. Therefore, the differences in the bacterial production rates between Davidson et al. (2013) and our data may be associated with inter-annual variability.

Our BGE ranged from 5 to 89%, in line with the range of BGEs compiled by del Giorgio and Cole (1998), the 11–75% reported by Catalano et al. (2014) in the Adriatic Sea, and the 3–71% range reported by Sintes et al. (2010) in the North Sea. However, the BGE are higher than the 5–28% range measured by Reinthaler and Herndl (2005) in the North Sea. The differences between the former estimates and those in the present study may be due to differing methodologies. Reinthaler and Herndl (2005) and Sintes et al. (2010) estimated bacterial respiration from dissolved oxygen consumption in pre-filtered samples incubated for 24 h, while our estimates are based on INT reduction in incubations lasting <2 h. Incubating pre-filtered water samples can lead to overestimates of bacterial respiration (Aranguren-Gassis et al., 2012), so that BGE in the former studies (Lemée et al., 2002; Reinthaler and Herndl, 2005; Sintes et al., 2010) may have been underestimated. However, our $INT_{0.2–0.8}$ rates, determined from samples filtered onto 0.2 µm filters could also be underestimated, due to the loss of bacterial cells less than 0.2 µm in diameter. Bacterial abundance in the 0.2 µm filtrate in July corresponded on average ($n = 7$) to 30 ± 2% of the BA in the unfiltered sample (data not shown). The percentage of bacteria passing through the 0.2 µm filter in this study is slightly higher than the 2–26% values reported by Gasol and Morán (1999). Thus, assuming a constant cell-specific respiration rate of all 0.2–0.8 µm bacteria, the bacterial respiration derived from $INT_{0.2–0.8}$ could be underestimated by ~30%. Recalculating BCD and BGE, using $INT_{0.2–0.8}$ increased by 30%, results in an increase in the monthly average BCD of the two stations (recalculated monthly average BCD: 359, 421 and 318 mg C m^{-2} d^{-1} in November, April and July, respectively) and a decrease in the monthly average BGE (recalculated monthly average BGE: 25%, 30% and 51% in November, April and July, respectively). Overall, the rates of plankton and bacterial metabolism measured here are comparable to previous rates measured in North Atlantic shelf seas (Supplementary Table 1).

4.3. Seasonal variability

The seasonal changes in environmental conditions occurring in the Celtic Sea (increased mixing in November, shallowing of the thermocline and development of a spring bloom in April and thermal stratification in July) was reflected in pronounced seasonality of CR_{O2} and BP in the UML. This seasonal variability in CR_{O2} and BP has been previously observed in coastal systems (Blight et al., 1995; Griffith and Pomeroy, 1995; Serret et al., 1999; Alonso-Sáez et al., 2008; Arbones et al., 2008; Céa et al., 2014). Highest CR_{O2} rates in the present study coincided with maximum values of primary production determined by uptake of radiolabelled bicarbonate (^{14}C-PP) in April (Fig. 9), and these two indicators of plankton metabolism were positively correlated ($r = 0.47$, $p < .0001$, $n = 72$). These observations are in agreement with previous seasonal studies where the highest respiration rates were measured during the time of highest phytoplankton abundance (Blight et al., 1995; Serret et al., 1999; Maixandeau et al., 2005; Arbones et al., 2008).

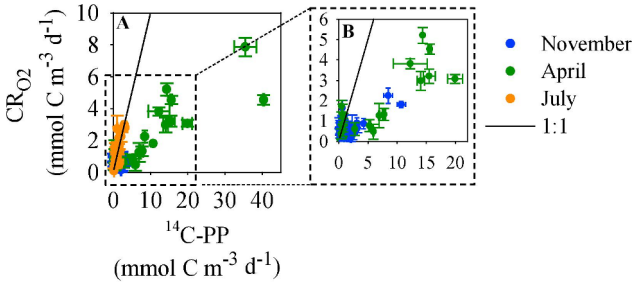

Fig. 9. Daily volumetric plankton community respiration (CR_{O2}) versus primary production determined from radiolabelled bicarbonate uptake after a 6–8 h incubation (^{14}C-PP) in November 2014 (blue), April 2015 (green) and July 2015 (orange) (A). (B) Zoom of the dotted area in (A) with November and April data only. Error bar represents the standard error and the solid line is the 1:1 line.

The relationship between ^{14}C-PP and CR_{O2} showed distinctive patterns in the three months, especially between April and July (Fig. 9). The linear regression slope between ^{14}C-PP and CR_{O2} was higher in July (0.78 ± 0.12), and statistically indistinguishable from unity (Clarke test, $t = 1.4$, $df = 35$, $p = .17$), while in April the slope was much lower (0.15 ± 0.02) and statistically different from unity (Clarke test, $t = 16$, $df = 70$, $p < .0001$). The difference in the ^{14}C-PP:CR_{O2} ratio indicates that the system was in metabolic balance during July, and acted as a sink of CO_2 and source of organic matter in April, with this surplus of organic matter consumed by bacteria and/or zooplankton, or transported horizontally or vertically. Minimum CR_{O2} values were measured in the Celtic Sea in November, despite the Chl-*a* concentrations being higher than in July, and the intermediate ^{14}C-PP rates measured during this month, meant that the system was net autotrophic (^{14}C-PP > CR_{O2}). Autotrophic conditions are not usually observed in November at this latitude (Blight et al., 1995; Serret et al., 1999). However, they might be related to our sampling of the late autumn plankton bloom phase that this area usually experiences (Martinez et al., 2011), as indicated by the environmental physico-chemical and biological conditions (Wihsgott et al., this issue). The high sea surface temperature, the presence of a thermocline at ~75 m and the low nutrient concentrations in the UML, all indicate that the water column was not completely mixed. In fact, data from a long-term mooring array situated at the CCS position indicated that there was an increase in Chl-*a* from late October until December 2014 indicative of an autumn bloom (Wihsgott et al., this issue). In addition, zooplankton abundance may have influenced the seasonal differences in the ^{14}C-PP:CR_{O2} ratio as intermediate CR_{O2} values were measured in July when Chl-*a* was lowest, but mesozooplankton (>200 µm) and nauplii abundances were high (Tarran et al., this issue; Giering et al., this issue). The low Chl-*a* values combined with the low $\%INT_{0.2–0.8}$ occurring in July support our suggestion that zooplankton had a higher contribution to CR_{O2} in July, leading to relatively high CR_{O2} rates.

In general, bacterial respiration only contributed 38%, 24% and 21% of the plankton community respiration in November, April and July, respectively. Despite the increase in production of organic matter by phytoplankton in April (Fig. 6, Poulton et al. this issue; Mayers et al. this issue), $INT_{0.2–0.8}$ did not show a corresponding increase. Several studies have suggested that bacterial respiration can be limited by concentrations of inorganic nitrogen or phosphorus (Rivkin and Anderson, 1997; Kirchman, 2000). However, since there was an increase in bacterial abundance and bacterial production, it seems that bacterial respiration was not limited by inorganic nutrients in our study. In fact, examination of inorganic phosphorus (P) uptake across the three sampling periods implied that while bacteria strongly influences P-uptake (and retention) in July, phytoplankton were more influential in April (Poulton et al., this issue). A possible explanation for the lack of a seasonal trend in bacterial respiration might be related to

seasonal changes in bacterial community composition (Gilbert et al., 2009, 2012; Tarran et al., this issue). Different bacterial groups may have different carbon compound requirements (Gómez-Consarnau et al., 2012), different respiration rates (del Giorgio and Gasol, 2008) and/or a differing ability to take up INT. The INT reduction technique has been used for a range of phytoplankton and bacterial cultures and natural samples (Martínez-García et al., 2009), but a comprehensive suite of culture experiments confirming that all representative groups of plankton and bacteria can equally take up and reduce INT has not yet taken place. Such experiments are required to confirm that $INT_{0.2–0.8}$ does not underestimate bacterial respiration when particular bacterial groups, which are less able to take up INT, are dominant.

The different seasonal evolution of $INT_{0.2–0.8}$, which decreased 2-fold from November and April to July, and bacterial production, which increased 2-fold from November to July, drove the changes in the seasonal variability in BCD and BGE. Published studies which have measured BGEs in temperate coastal regions all show seasonal variability (Lemée et al., 2002; Reinthaler and Herndl, 2005; Vázquez-Domínguez et al., 2007; Alonso-Sáez et al., 2008; Sintes et al., 2010, Céa et al., 2014), but there is no single environmental variable which consistently drives the variability in BGE. On the one hand, several researchers found that the seasonal variability in BGE was driven by changes in bacterial respiration (Sherry et al., 1999; Lemée et al., 2002; Vázquez-Domínguez et al., 2007), whereas other researchers concluded that bacterial production influenced the changes in BGE (del Giorgio and Cole, 2000; Reinthaler and Herndl, 2005). Similar to the seasonal study performed in the Bay of Marseille (Céa et al., 2014), the present study shows that the variability in both BP and $INT_{0.2–0.8}$ determined the variability of BGE. In our study, the two variables have different influences depending on the time of the year: BP was the dominant influence in November and April, while both BP and $INT_{0.2–0.8}$ drove the changes in July. However, this does not reveal which environmental conditions drive the changes in BP and $INT_{0.2–0.8}$, and therefore BGE. Production of dissolved organic carbon by phytoplankton did not control the changes in BGE and the relationships between environmental conditions (i.e. temperature and nutrient concentrations) and BGE were different in November, April and July. Differences in the quality of dissolved organic matter (DOM) observed in the Celtic Sea in 2014–15 (Davis et al., this issue) may explain some of the variability in the BGE. DOM was C-rich with high carbon:nitrogen (DOC:DON) ratios (average UML 16.6 ± 4.0) in April while in July the DOM was N-rich (average DOC:DON in the UML 11.0 ± 1.2) (Davis et al., this issue) when bacteria showed the highest bacterial production and lowest respiration rates. Bacteria must consume high quantities of carbon in high C:N ratio conditions in order to obtain enough nitrogen for production and growth (Linley and Newell, 1984) whereas under carbon limitation bacteria can take up N easily with a low C-respiration demand (Goldman et al., 1987; Kroer, 1993). This may explain our high BP rates associated with low $INT_{0.2–0.8}$ in July.

4.4. Consumption of phytoplankton produced dissolved organic carbon by bacteria

The release of DOC from phytoplankton is one of several interactions which exist between phytoplankton and bacteria (Cole, 1982, Amin et al., 2012). The organic carbon released by phytoplankton can be used as a substrate for bacteria (Cole, 1982; Baines and Pace, 1991; Morán et al., 2002), enhancing bacterial respiration and bacterial production (Blight et al., 1995; Alonso-Sáez et al., 2008). However, the consistent rates of bacterial respiration between November and April, despite a 3.8-fold greater average phytoplankton DOC production in the UML in April, and the lack of correlation between *p*DOC and $INT_{0.2–0.8}$, suggest that bacterial respiration in our study was not controlled by the availability of organic matter. On the contrary, the positive correlation between *p*DOC and bacterial production indicated that as *p*DOC increased the bacterial production increased, and so the local DOC produced by phytoplankton may have supported and stimulated the bacterial production. The use of organic compounds only for growth rather than for respiration means that respiration is less dependent on resources (López-Urrutia and Morán, 2007), and might be adopted as a survival response. For example, in April, when the inorganic nutrients start to decline due to phytoplankton uptake, and phytoplankton (the direct competitors for nutrients) dominated P-uptake (Poulton et al., this issue) and are increasing in number, bacteria could have used the *p*DOC to increase their production while respiration rates remained constant.

Previous studies have shown that during productive periods bacterial carbon requirements are sustained by concurrent phytoplankton DOC production, while external DOC inputs are required to fulfil the BCD during unproductive times (La Ferla et al., 2006; Alonso-Sáez et al., 2008; Catalano et al., 2014). In contrast to these results, in the present study *p*DOC was always higher than BCD, irrespective of the time of year (Fig. 6). Even if we consider that our BCD calculations are underestimated (see Section 4.2) and we recalculate the BCD with an increase of 30% in bacterial respiration, the *p*DOC was still greater (1–39-fold) than the recalculated BCD for all concurrent data. The *p*DOC:BCD > 1 suggests that bacterial metabolism was not limited by carbon availability, as there was always sufficient DOC produced by phytoplankton to satisfy the bacterial requirements. Therefore, phytoplankton and bacterial metabolism were coupled in terms of carbon, when “coupling” is considered to be the capacity of phytoplankton to produce enough dissolved organic carbon to fulfil the BCD (Morán et al., 2002). However, the magnitude of the bacterial carbon demand was not dependent on the amount of organic carbon produced by phytoplankton, as shown by the lack of relationship between *p*DOC and BCD within each month (Fig. 5). Morán et al. (2002) investigated the relationship between BCD and production of dissolved organic carbon in different ecosystems (Antarctic offshore, Antarctic coastal, NE Atlantic and NW Mediterranean), calculating BCD from bacterial production data collected in situ and assuming a constant BGE of 7.1, 15 and 30%. They concluded that the “*BCD would on average always exceed dissolved primary production in the NE Atlantic, unless unrealistically high BGEs were used*”. Contrary to their conclusion, our BCD values were always lower than the *p*DOC at a broad range of BGE values (5–89%) suggesting a good coupling between bacteria and phytoplankton.

4.5. Upper mixing layer versus bottom mixing layer

Light, nutrients, phytoplankton biomass, and community structure may have a major control on plankton metabolism in the UML and BML. In general, the BML was characterized by low light intensities (< 0.1% of the I_0), lower temperatures and higher nutrient concentrations. The temperature difference between the two layers was < 1 °C in November and April and ~2.5 °C in July. Bacterial metabolism is positively related to temperature (Kirchman et al., 2005; Vázquez-Domínguez et al., 2007; Kritzberg et al., 2010). However, we found similar cell-specific bacterial respiration rates in the UML and BML and no relationship between temperature and BP.

CR_{O2} and BP were higher in the UML than in the BML (4-fold and 7-fold, respectively) presumably as a result of the larger amount of phytoplankton and bacteria in the UML than the BML. Our community respiration results contrast with a previous study undertaken in the Adriatic Sea (Catalano et al., 2014) where despite the higher phytoplankton and bacterial abundance in the UML compared to the BML, the community respiration was 5-fold greater in the BML. However, our BP agrees with the higher BP rates in the UML observed in the Adriatic Sea (Catalano et al., 2014). In our study, there were differences in the DOM concentration between the two layers, with higher concentrations of DOC in April, and DON in July in the UML compared to the BML (Davis et al., this issue), and these differences could have contributed to the higher bacterial production in the UML. However, $INT_{0.2–0.8}$ and cell-specific bacterial respiration rates were similar in both layers

suggesting that the interactions between phytoplankton and bacteria were favouring bacterial production in the UML and not bacterial respiration. Overall, our results contrast with a previous study in the North Sea, which reported a separation in the water column of consumption of dissolved inorganic carbon (DIC; primary production), which occurred in the surface layers, from DIC production (respiration) which occurred in the bottom mixed waters (Thomas et al., 2004). In this former study, the enhancement of respiration processes below the UML during a stratified period increased the transport of CO_2 from the shelf sea to the open ocean (Thomas et al., 2004). In contrast to Thomas et al. (2004), our results suggest that most of the respiratory CO_2 production occurred in the UML of the water column, contributing to the CO_2 available for evasion to the atmosphere rather than export via advection to the open sea.

5. Conclusion

Pronounced seasonal variability was observed in the Celtic Sea, with higher rates of plankton community respiration at the end of April, highest rates of bacterial production and bacterial growth efficiency in July, and lowest rates of CR_{O2}, BP and BGE in November. The relationship between plankton community respiration and primary production differed between seasons, with ^{14}C-PP > CR_{O2} in April as a result of the phytoplankton bloom and ^{14}C-PP ~ CR_{O2} during July, due to the combination of lower ^{14}C-PP and higher CR_{O2}. Comparison of the rates of plankton metabolism in the UML with those in the BML indicated greater variability and higher rates in community respiration and bacterial production in the UML than in the BML. However, bacterial respiration was similar in both layers. This constancy in the bacterial respiration rates might be explained by a lack of dependency of bacterial respiration on the production of dissolved organic carbon or/and by a difference in bacterial community composition. The inner Shelf Sea and the Shelf Edge had similar rates of carbon cycling except in April when more organic carbon was produced in the inner Shelf Sea which could be exported to deeper areas. Our data clearly demonstrate that bacterial growth efficiency varies with season and depth as a response to the greater variability in bacterial production than in respiration. Inclusion of this variability in BGE in future studies or model simulations is necessary for realistic carbon budget calculations as estimates of the production of CO_2 by bacteria derived using a constant BGE could incur significant biases.

Acknowledgements

We thank the captains and crew of the *RRS Discovery* for their help and support at sea and all the scientists involved in the three cruises. We would also like to thank Jo Hopkins and Charlotte Williams (National Oceanographic Centre, Liverpool) for assistance and provision of the physical characterization of the area, Malcolm Woodward and Carolyn Harris for nutrient analyses, Clare Ostle and Jose Lozano for assistance with the dissolved oxygen measurements (November cruise and April cruise, respectively), Callum White and Elaine Mitchel for assistance with bacterial production measurements (April cruise) and Ray Leakey for advice on bacterial production methodology and data analysis. We are grateful to the UK Natural Environment Research Council (NERC) for funding the research cruises via the Shelf Sea Biogeochemistry program. The data are publicly available under the NERC Open Government Licence: http://www.bodc.ac.uk/data/documents/nodb/267802/.

E.EG-M was funded by NERC grant NE/K00168X/1 (awarded to C. Robinson and D. A. Purdie) and by a research grant from The Leverhulme Trust (RPG-2017-089 awarded to UEA) during the writing of this paper. SM was funded by NERC grant NE/K001884/1 (awarded to K. Davidson). GAT was funded by NERC grant NE/K002058/1. KMJM, AJP and CJD were funded by NERC grant NE/K001701/1 (awarded to A.J. Poulton). CED and CM were funded by NERC grant NE/K002007/1 (awarded to C. Mahaffey).

Appendix A. Supplementary material

Supplementary data associated with this article can be found, in the online version, at http://dx.doi.org/10.1016/j.pocean.2017.12.002.

References

Alonso-Sáez, L., Vázquez-Domínguez, E., Cardelús, C., Pinhassi, J., Sala, M., Lekunberri, I., Balagué, V., Vila-Costa, M., Unrein, F., Massana, R., Simó, R., Gasol, J., 2008. Factors controlling the year-round variability in carbon flux through bacteria in a coastal marine system. Ecosystems 11, 397–409.

Amin, S.A., Parker, M.S., Armbrust, E.V., 2012. Interactions between diatoms and bacteria. Microbiol. Mol. Biol. Rev. 76, 667–684.

Aranguren-Gassis, M., Teira, E., Serret, P., Martínez-García, S., Fernández, E., 2012. Potential overestimation of bacterial respiration rates in oligotrophic plankton communities. Mar. Ecol. Prog. Ser. 453, 1–10.

Arbones, B., Castro, C.G., Alonso-Perez, F., Figueiras, F.G., 2008. Phytoplankton size structure and water column metabolic balance in a coastal upwelling system: the Ría de Vigo, NW Iberia. Aquat. Microb. Ecol. 50, 169–179.

Baines, S.B., Pace, M.L., 1991. The production of dissolved organic matter by phytoplankton and its importance to bacteria: patterns across marine and freshwater systems. Limnol. Oceanogr. 36, 1078–1090.

Blight, S., Bentley, T., Lefevre, D., Robinson, C., Rodrigues, R., Rowlands, J., Williams, P.J le B., 1995. Phasing of autotrophic and heterotrophic plankton metabolism in a temperate coastal ecosystem. Mar. Ecol. Prog. Ser. 128, 61–75.

Carlson, C.A., Hansell, D.A., Nelson, N.B., Siegel, D.A., Smethie, W.M., Khatiwala, S., Meyers, M.M., Halewood, E., 2010. Dissolved organic carbon export and subsequent remineralization in the mesopelagic and bathypelagic realms of the North Atlantic basin. Deep Sea Res. Part II 57, 1433–1445.

Carritt, D.E., Carpenter, J.H., 1966. Comparison and evaluation of currently employed modifications of the Winkler method for determining dissolved oxygen in seawater; a NASCO Report. J. Mar. Res. 24, 286–319.

Catalano, G., Azzaro, M., Bastianini, M., Bellucci, L.G., Bernardi Aubry, F., Bianchi, F., Burca, M., Cantoni, C., Caruso, G., Casotti, R., Cozzi, S., Del Negro, P., Fonda Umani, S., Giani, M., Giuliani, S., Kovacevic, V., La Ferla, R., Langone, L., Luchetta, A., Monticelli, L.S., Piacentino, S., Pugnetti, A., Ravaioli, M., Socal, G., Spagnoli, F., Ursella, L., 2014. The carbon budget in the northern Adriatic Sea, a winter case study. J. Geophys. Res. Biogeosci. 119, 1399–1417.

Céa, B., Lefèvre, D., Chirurgien, L., Raimbault, P., Garcia, N., Charrière, B., Grégori, G., Ghiglione, J.F., Barani, A., Lafont, M., Van Wambeke, F., 2014. An annual survey of bacterial production, respiration and ectoenzyme activity in coastal NW Mediterranean waters: temperature and resource controls. Environ. Sci. Pollut. Res. 22, 13654–13668.

Clarke, M.R.B., 1980. The reduced major axis of a bivariate sample. Biometrika 67, 441–446.

Cole, J.J., 1982. Interactions between bacteria and algae in aquatic ecosystems. Annu. Rev. Ecol. Syst. 13, 291–314.

Davidson, K., Gilpin, L.C., Pete, R., Brennan, D., McNeill, S., Moschonas, G., Sharples, J., 2013. Phytoplankton and bacterial distribution and productivity on and around Jones Bank in the Celtic Sea. Prog. Oceanogr. 117, 48–63.

Davis, C.E., Mahaffey, C., Wolf, G., Sharples, J., 2017;al., this issue. What's the matter: Seasonal organic matter dynamics across a temperate shelf sea. Prog. Oceanogr (This issue).

De Haas, H., Van Weering, T.C., De Stigter, H., 2002. Organic carbon in shelf seas: sinks or sources, processes and products. Cont. Shelf Res. 22, 691–717.

Del Giorgio, P.A., Cole, J.J., 1998. Bacterial growth efficiency in natural aquatic systems. Annu. Rev. Ecol. Syst. 503–541.

Del Giorgio, P.A., Cole, J.J., 2000. Bacterial Energetics and Growth Efficiency. Microbial Ecology of the Oceans. Wiley-Liss, pp. 289–325.

Del Giorgio, P.A., Gasol, J.M., 2008. Physiological Structure and Single-cell Activity in Marine Bacterioplankton. In: Kirchman, D.L. (Ed.), Microbial Ecology of the Oceans. John Wiley & Sons Inc, pp. 243–298.

Elser, J.J., Stabler, L.B., Hassett, R.P., 1995. Nutrient limitation of bacterial growth and rates of bacterivory in lakes and oceans: a comparative study. Aquat. Microb. Ecol. 9, 105–110.

García-Martín, E.E., Daniels, C.J., Davidson, K., Lozano, J., Mayers, K.M.J., McNeill, S., Mitchell, E., Poulton, A.J., Purdie, D.A., Tarran, G.A., Whyte, C., Robinson, C., 2017;al., this issue. Plankton community respiration and bacterial metabolism in a North Atlantic Shelf Sea during spring bloom development (April 2015). Prog. Oceanogr (This issue).

Gasol, J.M., Morán, X.A.G., 1999. Effects of filtration on bacterial activity and picoplankton community structure as assessed by flow cytometry. Aquat. Microb. Ecol. 16, 251–264.

Giering, S.L.C., Wells, S.R., Mayers, K.M.J., Tarran, G.A., Cornwell, L., Fileman, E., Atkinson, A., Mayor, D.J., 2017;al., this issue. Seasonal changes in zooplankton biomass, community composition and stoichiometry in the UK Shelf Sea. Prog. Oceanogr This issue.

Gilbert, J.A., Field, D., Swift, P., Newbold, L., Oliver, A., Smyth, T., Somerfield, P.J., Huse, S., Joint, I., 2009. The seasonal structure of microbial communities in the Western English Channel. Environ. Microbiol. 11, 3132–3139.

Gilbert, J.A., Steele, J.A., Caporaso, J.G., Steinbrück, L., Reeder, J., Temperton, B., Huse, S., Mchardy, A.C., Knight, R., Joint, I., 2012. Defining seasonal marine microbial community dynamics. ISME J. 6, 298–308.

Goldman, J.C., Caron, D.A., Dennett, M.R., 1987. Regulation of gross growth efficiency

and ammonium regeneration in bacteria by substrate C: N ratio. Limnol. Oceanogr. 32, 1239–1252.
Gómez-Consarnau, L., Lindh, M.V., Gasol, J.M., Pinhassi, J., 2012. Structuring of bacterioplankton communities by specific dissolved organic carbon compounds. Environ. Microbiol. 14, 2361–2378.
Griffith, P.C., Pomeroy, L.R., 1995. Seasonal and spatial variations in pelagic community respiration on the southeastern US continental shelf. Cont. Shelf Res. 15, 815–825.
Herndl, G.J., Reinthaler, T., 2013. Microbial control of the dark end of the biological pump. Nat. Geosci. 6, 718–724.
Hickman, A.E., Moore, C., Sharples, J., Lucas, M.I., Tilstone, G.H., Krivtsov, V., Holligan, P.M., 2012. Primary production and nitrate uptake within the seasonal thermocline of a stratified shelf sea. Mar. Ecol. Prog. Ser. 463, 39–57.
Hickman, A., Poulton, A.J., Mayers, K.M.J., Tarran, G.A., 2017;al., this issue. Seasonal variability in size-fractionated chlorophyll-a and primary production in the Celtic Sea. Prog. Oceanogr This issue.
Humphreys, M.P., Moore, C.M., Achterberg, E.P., Griffiths, A.M., Smilenova, A., Hartman, S.E., Kivimäe, C., Woodward, E.M.S., Hopkins, J.E., 2017;al., this issue. Balancing the inorganic carbon and nutrient budgets in a seasonally-stratifying temperate shelf sea. Prog. Oceanogr This issue.
Hydes, D.J., Le Gall, A.C., Miller, A.E.J., Brockmann, U., Raabe, T., Holley, S., Alvarez-Salgado, X., Antia, A., Balzer, W., Chou, L., Elskens, M., Helder, W., Joint, I., Orren, M., 2001. Supply and demand of nutrient and dissolved organic matter at and across the N.W. European shelf break in relation to hydrography and biogeochemical activity. Deep-Sea Res. Part II 48, 3023–3047.
Joint, I., Owens, N., Pomroy, A., 1986. Seasonal production of photosynthetic picoplankton and nanoplankton in the Celtic Sea. Mar. Ecol. Prog. Ser. 28, 251–258.
Joint, I., Pomroy, A., 1987. Activity of heterotrophic bacteria in the euphotic zone of the Celtic Sea. Mar. Ecol. Prog. Ser. 41, 155–165.
Joint, I., Wollast, R., Chou, L., Batten, S., Elskens, M., Edwards, E., Hirst, A., Burkill, P., Groom, S., Gibb, S., 2001. Pelagic production at the Celtic Sea shelf break. Deep Sea Res. Part II 48, 3049–3081.
Kirchman, D., 2001. Measuring bacterial biomass production and growth rates from leucine incorporation in natural aquatic environments. Method. Microbiol. 30, 227–237.
Kirchman, D.L., 2000. Uptake and regeneration of inorganic nutrients by marine heterotrophic bacteria. In: Kirchman, D.L. (Ed.), Microbial Ecology of the Oceans. Wiley, pp. 261–288.
Kirchman, D.L., Malmstrom, R.R., Cottrell, M.T., 2005. Control of bacterial growth by temperature and organic matter in the Western Arctic. Deep-Sea Res. Part II-Top. Stud. Oceanogr. 52, 3386–3395.
Kritzberg, E.S., Duarte, C.M., Wassmann, P., 2010. Changes in Arctic marine bacterial carbon metabolism in response to increasing temperature. Polar Biol. 33, 1673–1682.
Kroer, N., 1993. Bacterial growth efficiency on natural dissolved organic matter. Limnol. Oceanogr. 38, 1282–1290.
La Ferla, R., Azzaro, M., Maimone, G., 2006. Microbial respiration and trophic regimes in the Northern Adriatic Sea (Mediterranean Sea). Estuar. Coast. Shelf Sci. 69, 196–204.
Lee, C.W., Bong, C.W., Hii, Y.S., 2009. Temporal variation of bacterial respiration and growth efficiency in tropical coastal waters. Appl. Environ. Microbiol. 75, 7594–7601.
Legendre, L., Rivkin, R.B., Weinbauer, M.G., Guidi, L., Uitz, J., 2015. The microbial carbon pump concept: potential biogeochemical significance in the globally changing ocean. Prog. Oceanogr. 134, 432–450.
Legendre, P., Anderson, M.J., 1999. Distance-based redundancy analysis: testing multispecies responses in multifactorial ecological experiments. Ecol. Monogr. 69, 1–24.
Lemée, R., Rochelle-Newall, E., Van Wambeke, F., Pizay, M.D., Rinaldi, P., Gattuso, J.P., 2002. Seasonal variation of bacterial production, respiration and growth efficiency in the open NW Mediterranean Sea. Aquat. Microb. Ecol. 29, 227–237.
Li, W., Dickie, P., Harrison, W., Irwin, B., 1993. Biomass and production of bacteria and phytoplankton during the spring bloom in the western North Atlantic Ocean. Deep Sea Res. Part II 40, 307–327.
Linley, E., Newell, R., 1984. Estimates of bacterial growth yields based on plant detritus. Bull. Mar. Sci. 35, 409–425.
Longnecker, K., Sherr, B., Sherr, E., 2006. Variation in cell-specific rates of leucine and thymidine incorporation by marine bacteria with high and with low nucleic acid content off the Oregon coast. Aquat. Microb. Ecol. 43, 113–125.
López-Sandoval, D., Fernández, A., Marañón, E., 2011. Dissolved and particulate primary production along a longitudinal gradient in the Mediterranean Sea. Biogeosciences 8, 815–825.
López-Urrutia, Á., Morán, X.A.G., 2007. Resource limitation of bacterial production distorts the temperature dependence of oceanic carbon cycling. Ecology 88, 817–822.
Maixandeau, A., Lefèvre, D., Fernández, I.C., Sempere, R., Sohrin, R., Ras, J., Van Wambeke, F., Caniaux, G., Quéguiner, B., 2005. Mesoscale and seasonal variability of community production and respiration in the surface waters of the NE Atlantic Ocean. Deep-Sea Res. Part I-Oceanogr. Res. Pap. 52, 1663–1676.
Marra, J., 2002. Approaches to the measurement of plankton production. In: Williams, P.J.le B., Thomas, D.N., Reynolds, C.S. (Eds.), Phytoplankton Productivity: Carbon Assimilation in Marine and Freshwater Ecosystems. Blackwell, Cambridge, U.K., pp. 78–108.
Martin-Jézéquel, V., Videau, C., 1992. Phytoplankton and bacteria over the transient area of the continental slope of the Celtic Sea in spring. I. Vertical distribution and productivity. Mar. Ecol. Prog. Ser. 85, 289–301.
Martinez, E., Antoine, D., D'ortenzio, F., De Boyer Montégut, C., 2011. Phytoplankton spring and fall blooms in the North Atlantic in the 1980s and 2000s. J. Geophys. Res. Oceans 116.
Martínez-García, S., Fernández, E., Aranguren-Gassis, M., Teira, E., 2009. In vivo electron transport system activity: a method to estimate respiration in natural marine microbial planktonic communities. Limnol. Oceanogr.: Methods 7, 459–469.
Mayers, K.M.J., Poulton, A.J., Daniels, C.J., Wells, S.R., Woodward, E.M.S., Tyrrell, T., Giering, S.L.C., 2017;al., this issue. Top-down control of coccolithophore populations during spring in a temperate Shelf Sea (Celtic Sea, April 2015). Prog. Oceanogr This issue.
Miller, J.C., Miller, J.N., 1988. Statistics for Analytical Chemistry, 2nd ed. Ellis Horwood, Chichester.
Moore, C.M., Suggett, D.J., Hickman, A.E., Kim, Y.-N., Tweddle, J.F., Sharples, J., Geider, R.J., Holligan, P.M., 2006. Phytoplankton photoacclimation and photoadaptation in response to environmental gradients in a shelf sea. Limnol. Oceanogr. 51, 936–949.
Morán, X.A.G., Estrada, M., Gasol, J.M., Pedrós-Alió, C., 2002. Dissolved primary production and the strength of phytoplankton–bacterioplankton coupling in contrasting marine regions. Microbiol. Ecol. 44, 217–223.
Pingree, R.D., 1980. Physical Oceanography of the Celtic Sea and English Channel. In: Banner, M.B.C.F.T., Massie, K.S. (Eds.), The North-West European Shelf Seas: The Sea Bed and the Sea in Motion II. Physical and Chemical Oceanography, and Physical Resources. Elsevier, pp. 415–465.
Pingree, R., Griffiths, D., Mardell, G., 1983. The structure of the internal tide at the Celtic Sea shelf break. J. Mar. Biol. Assoc. United Kingdom 64, 99–113.
Pomroy, A., Joint, I., 1999. Bacterioplankton activity in the surface waters of the Arabian Sea during and after the 1994 SW monsoon. Deep Sea Res. Part II 46, 767–794.
Poulton, A.J., Daniels, C.J., Esposito, M., Humphreys, M.P., Mitchell, E., Ribas-Ribas, M., Russell, B.C., Stinchcombe, M.C., Tynan, E., Richier, S., 2016. Production of dissolved organic carbon by Arctic plankton communities: Responses to elevated carbon dioxide and the availability of light and nutrients. Deep Sea Res. Part II 127, 60–74.
Poulton, A.J., Davis, C.E., Daniels, C.J., Mayers, K.M.J., Harris, C., Tarran, G.A., Widdicombe, C.E., Woodward, E.M.S., 2017;al., this issue. Seasonal phosphorus dynamics in a temperate shelf sea (Celtic Sea): uptake, release, turnover and stoichiometry. Prog. Oceanogr This issue.
Reinthaler, T., Herndl, G.J., 2005. Seasonal dynamics of bacterial growth efficiencies in relation to phytoplankton in the southern North Sea. Aquat. Microb. Ecol. 39, 7–16.
Rivkin, R.B., Anderson, M.R., 1997. Inorganic nutrient limitation of oceanic bacterioplankton. Limnol. Oceanogr. 42, 730–740.
Robinson, C., Tilstone, G.H., Rees, A.P., Smyth, T.J., Fishwick, J.R., Tarran, G.A., Luz, B., Barkan, E., David, E., 2009. Comparison of in vitro and in situ plankton production determinations. Aquat. Microb. Ecol. 54, 13–34.
Serret, P., Fernández, E., Sostres, J.A., Anadón, R., 1999. Seasonal compensation of microbial production and respiration in a temperate sea. Mar. Ecol. Prog. Ser. 187, 43–57.
Sharples, J., Mayor, D.J., Poulton, A.J., Rees, A.P., Robinson, C., 2017;al., this issue. Why do shelf seas not run out of nutrients? Prog. Oceanogr This issue.
Sharples, J., Moore, C.M., Hickman, A.E., Holligan, P.M., Tweddle, J.F., Palmer, M.R., Simpson, J.H., 2009. Internal tidal mixing as a control on continental margin ecosystems. Geophys. Res. Lett. 36, L23603. http://dx.doi.org/10.1029/2009gl040683.
Sharples, J., Moore, M.C., Rippeth, T.P., Holligan, P.M., Hydes, D.J., Fisher, N.R., Simpson, J.H., 2001. Phytoplankton distribution and survival in the thermocline. Limnol. Oceanogr. 46, 486–496.
Sherry, N.D., Boyd, P.W., Sugimoto, K., Harrison, P.J., 1999. Seasonal and spatial patterns of heterotrophic bacterial production, respiration, and biomass in the subarctic NE Pacific. Deep Sea Res. Part II 46, 2557–2578.
Sintes, E., Stoderegger, K., Parada, V., Herndl, G.J., 2010. Seasonal dynamics of dissolved organic matter and microbial activity in the coastal North Sea. Aquat. Microb. Ecol. 60, 85.
Tarran, G.A., Heywood, J.L., Zubkov, M.V., 2006. Latitudinal changes in the standing stocks of nano- and picoeukaryotic pytoplankton in the Atlantic Ocean. Deep Sea Res. Part II 53, 1516–1529.
Tarran, G.A., Hickman, A.E., Poulton, A.J., Widdicombe, C.E., Rees, A.P., Fox, J.E., Munns, L., 2017;al., this issue. European Shelf Sea phyto- and microplankton: communities, abundance and seasonality in the Celtic Sea. Prog. Oceanogr (This issue).
Thomas, H., Bozec, Y., Elkalay, K., De Baar, H.J., 2004. Enhanced open ocean storage of CO_2 from shelf sea pumping. Science 304, 1005–1008.
Vázquez-Domínguez, E., Vaqué, D., Gasol, J.M., 2007. Ocean warming enhances respiration and carbon demand of coastal microbial plankton. Glob. Change Biol. 13, 1327–1334.
Woodward, E.M.S., Rees, A.P., 2001. Nutrient distributions in an anticyclonic eddy in the northeast Atlantic Ocean, with reference to nanomolar ammonium concentrations. Deep Sea Res. Part II 48 (4), 775–793.
Wihsgott, J.U., Sharples, J., Hopkins, J.E., Woodward, E.M.S., Greenwood, N., Hull, T., Sivyer, D.B., 2017;al., this issue. Investigating the autumn bloom's significance within the seasonal cycle of primary production in a temperate shelf sea. Prog. Oceanogr (This issue).